JPIS (Jurnal Pendidikan Ilmu Sosial)

Journal homepage: https://ejournal.upi.edu/index.php/jpis

Analyzing the Impact of Calibration Parameters on Ground Control Point's Error Ellipses in Orthophotos

Anisa Nabila Rizki Ramadhani[1], Komang Bayu Angga Sardana[2]
[1]Program Studi Survei Pemetaan dan Informasi Geografis, Universitas Pendidikan Indonesia
[2]Pusat Pendidikan Topografi, Direktorat Topografi Angkatan Darat
Correspondence: E-mail: anisanabilarr@upi.edu

ABSTRACT

Orthophoto accuracy is strongly influenced by camera calibration parameters and the spatial distribution of Ground Control Points (GCPs). However, the interaction between these factors remains insufficiently explored, especially using spatial error representations such as error ellipses. This study addresses that gap by analyzing how intrinsic camera parameters affect spatial accuracy in relation to varied GCP configurations. Aerial data were collected over twelve sample locations within the Indonesian University of Education campus. Positional errors were evaluated through two- and three-dimensional error ellipses, with correlation analyses performed between maximum GCP errors and individual calibration parameters. The results reveal prosibilities of correlations between calibration quality and error magnitude. High focal length stability and minimal principal point offset were associated with lower errors, while increased radial and tangential distortion often led to spatial inaccuracy. Anomalies were observed, highlighting the sensitivity of orthophoto precision to calibration deviations and poor GCP layouts. Correlation analysis revealed that a deviation of >50 pixels in the principal point coordinate is associated with an increase of up to 35 cm in spatial error This study emphasizes the importance of stable calibration and optimal GCP distribution in minimizing positional uncertainty.

ARTICLE INFO

Article History:
Submitted/Received 02 Jun 2025
First Revised 05 Agst 2025
Accepted 21 Sept 2025
First Available online 30 Dec 2025
Publication Date 30 Dec 2025

Keyword:
Calibration Parameters, Error Ellipses, Residual Errors, Orthophotos, Photogrammetry, Ground Control Points (GCPs).

1. INTRODUCTION

Photogrammetry is a widely used technique in remote sensing and geospatial analysis for extracting accurate geometric information from aerial or satellite imagery (Gui, 2024 ; Colombia, 2014 ; Fotlani, 2018 ; Burdziakowski, 2020 ; Bolkas, 2023). One of its key products is the orthophoto, a geometrically corrected image that represents the Earth's surface with uniform scale (Şahin, 2023). Orthophotos are essential for various applications such as topographic mapping, land use planning, environmental monitoring, and infrastructure development (Kaamin, 2023). The geometric accuracy of orthophotos is crucial, especially when they are used for high-precision tasks like cadastral mapping or engineering design. Ground Control Points (GCPs) are physical points with known coordinates used to georeference images and ensure spatial accuracy. The quality and distribution of GCPs significantly influence the precision of orthophoto generation (Garcia, 2020 ; pessona, 2020 ; Sanz-Ablanedo, 2018). Camera calibration is a critical step in photogrammetric processing, where intrinsic and extrinsic parameters of the imaging system are estimated. Poor calibration can lead to systematic distortions in image geometry (Zhang Y. C., 2023) (Kshirsagar, 2024). Additionally, residual errors, which are the differences between observed and predicted image positions of points, reflect inaccuracies in the photogrammetric model and adjustment process. Error ellipses are graphical representations of positional uncertainty in the horizontal plane. They provide insights into the quality and reliability of derived coordinates, often used to assess the spatial precision of GCPs in the resulting orthophotos. While previous studies (Hageman, 2021 ; Shortis, 1998 ; Bolkas, 2020 ; Xhpu, 2020 ; Maalek, 2020). have focused on the influence of GCP distribution or quantity on orthophoto accuracy, less attention has been given to how camera calibration quality and residual errors affect the shape and orientation of error ellipses, and the correlation structure between GCPs. Understanding these relationships is essential for optimizing photogrammetric workflows. This study is novel in its integration of two- and three-dimensional error ellipse modeling with a multivariate analysis of intrinsic camera parameters—an approach rarely employed in UAV-based photogrammetry research. It aims to analyze how variations in calibration quality and residual error patterns influence the characteristics of error ellipses and the statistical correlation among GCPs in orthophoto generation (Viswanathan, 2005).

2. LITERATURE REVIEW AND METHODS

This study was conducted within the campus area of the Indonesian University of Education, utilizing twelve strategically selected sample locations to represent variations in the distribution of Ground Control Points (GCPs) and to assess the influence of camera calibration parameters on spatial accuracy. The selected locations included a combination of identical and differing GCP configurations to evaluate the variability of calibration impacts on error distribution, as visualized through error ellipses. At each location, both the number and spatial pattern of GCPs were deliberately varied. This was intended to analyze how different quantities and arrangements of GCPs affect the accuracy of orthophoto generation, particularly in terms of the spatial precision represented by error ellipses (Skarlatos, 2021 ; Seo, 2021 ; Gindraux, 2017 ; Zhao, 2021). The study aimed to examine the relationship between the quality of GCP configuration and the magnitude of residual errors resulting from the image rectification process

DOI: https://doi.org/10.17509/jpis.v32i1.55969
e-ISSN: 2540-7694 |p-ISSN: 0854-5251

The core analysis focused on four key camera calibration parameters: focal length, principal point, radial distortion coefficients, and tangential distortion coefficients. These parameters were calculated and subsequently assessed in relation to the maximum positional errors along the x and y axes. These positional errors were then translated into elliptical error representations as a means of quantifying positional uncertainty.

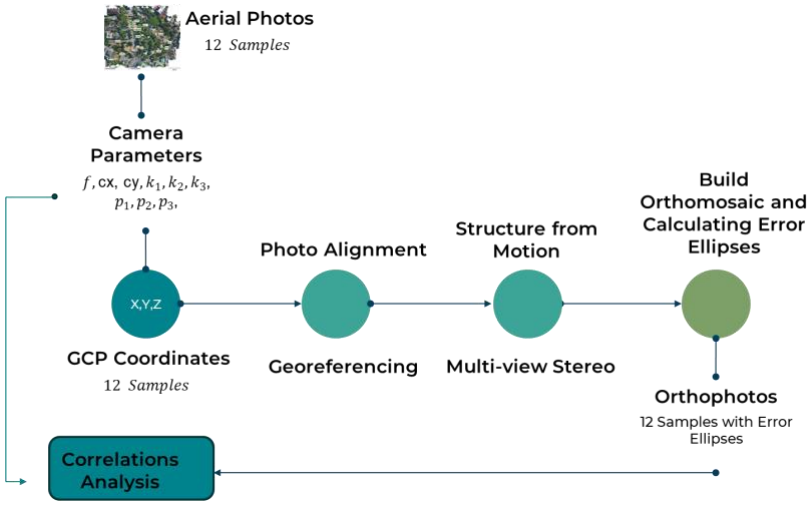

Flow Diagram 1. Illustration of Methodologies

The error ellipses were visualized in both two-dimensional and three-dimensional spaces, incorporating the x, y, and z components, to provide a comprehensive understanding of the spatial relationships among GCPs based on their field configurations. Correlation analysis was then employed to explore the relationship between the calibration parameters and the size and orientation of the error ellipses. The results of this analysis are expected to yield a deeper understanding of the extent to which calibration quality and GCP distribution patterns influence the geometric accuracy of orthophoto products.

2.1. Analytical Self-Calibration

Camera calibration parameters, often referred to as elements of interior orientation, are critical factors that must be considered to achieve accurate photogrammetric measurements (Yusoff M. Z., 2017). For metric cameras, these distortion parameters generally remain stable over extended periods, reducing the frequency of calibration needs, although periodic calibration is recommended according to the manufacturer's guidelines. In contrast, nonmetric cameras typically exhibit variability in their calibration parameters even between different usage sessions (Fryskowska, 2016 ; Campos, 2015 ; Morgan, 2014). Nevertheless, through the application of analytical self-calibration techniques, nonmetric cameras are frequently capable of delivering highly precise measurement results (Rokhmana, 2019). There is no assurance that the calibration parameters will remain consistent during field operations, as internal mechanical components of the camera may shift between the time of calibration and image acquisition (Tjahjadi, 2019 ; Sobura, 2021 ; Yusoff A. R., 2015 ; Qiang, 2016). Analytical self-calibration addresses this issue by enhancing the standard collinearity equations with additional terms that allow for the adjustment of the calibrated focal length, principal point offsets, as well as symmetric radial and decentering lens distortions (Fraser, 2006 ; Lichti, 2005 ; Brown, 1971 ; Zhang Z. , 2000). Furthermore, these equations can be expanded to include corrections for atmospheric refraction effects. The traditional form of these augmented collinearity equations is illustrated as follows:

DOI: https://doi.org/10.17509/jpis.v32i1.55969
e-ISSN: 2540-7694 p-ISSN: 0854-5251

$$x_a = x_0 - \overline{x}_a(k_1 r_a^2 + k_2 r_a^4 + k_3 r_a^6) + (1 + p_3 r_a^2) + \left[p_1\left(2\overline{x}_a^2 + r_a^2\right) + 2p_2 \overline{x}_2 \overline{y}_2\right] - f\frac{r}{q} \quad (1)$$

$$y_a = y_0 - \overline{y}_a(k_1 r_a^2 + k_2 r_a^4 + k_3 r_a^6) + (1 + p_3 r_a^2) + \left[2p_1 \overline{x}_a \overline{y}_a + p_2(2\overline{y}_a^2 + r_a^2\right] - f\frac{s}{q} \quad (2)$$

Where

$x_a, y_a = measured\ photo\ coordinates\ related\ to\ fiducials$
$x_0, y_0 = coordinates\ of\ the\ principal\ point$
$\overline{x}_a = x_a - x_0$
$\overline{y}_a = y_a - y_0$
$r_a^2 = \overline{x}_a^2 + \overline{y}_a^2$
$k_1, k_2, k_3 = symmetric\ radial\ lens\ distortion\ coefficients$
$p_1, p_2, p_3 = dicentering\ distortion\ coefficients$
$f = calibrated\ focal\ length$
$r, s, p = collinearity\ equation$

2.2 Ellipse Error Analysis

Error ellipses give a two-dimentional representation of the uncertainties of the adjusted coordinates of points as determined in a least squares adjustment (Ghilani, 2018 ; Mikhail, 1981). In photogrammetric analysis, the precision of determining spatial coordinates from aerial or ground-based images is influenced by various uncertainties inherent in the measurement process. A widely adopted approach to express and evaluate these positional uncertainties is through error ellipses. These ellipses serve as both a visual and quantitative tool to represent the accuracy of points obtained through photogrammetric techniques, including Ground Control Points (GCPs) and tie points (Okie, 2020 ; Šidák, 1967).

An error ellipse defines a confidence region around a measured point, indicating the area within which the true location is statistically expected to be found, commonly at confidence levels such as 95%. The ellipse's dimensions, shape, and orientation convey the error covariance and correlation in the horizontal plane, offering critical information on the scale and directional tendencies of spatial errors. This method plays a vital role in assessing the quality of photogrammetric outputs, facilitating quality assurance, and optimizing camera calibration and image orientation workflows. By analyzing error ellipses, practitioners can better understand the accuracy and reliability of spatial data, make informed adjustments to processing parameters, and enhance the geometric fidelity of products such as orthophotos and digital terrain models. The equations to visualize ellipse error shown below:

Calculating the standard deviation of X (σx)

$\sigma x = \sqrt{\sigma_x^2}$ (3) where $\sigma x\ is\ standar\ deviation\ of\ x$

Calculating the standard deviation of Y(σy)

$\sigma y = \sqrt{\sigma_y^2}$ (4) where σy is standard deviation of y

Calculating the variance of X ($\sigma^2 x$)and Y($\sigma^2 y$)

$\sigma_x^2 = \frac{\sum_{i=1}^{n}(x_i - \overline{x})^2}{n}$ (5)

where $x_i\ is\ coordinate\ of\ x, \overline{x}\ is\ the\ average\ of\ coordinate\ x, and\ n\ is\ total\ data$

DOI: https://doi.org/10.17509/jpis.v32i1.55969
e-ISSN: 2540-7694 |p-ISSN: 0854-5251

and $\sigma_y^2 = \frac{\sum_{i=1}^{n}(y_i-\overline{y})^2}{n}$ (6)

where y_i *is coordinate of* $y, \overline{y}$ *is the average of coordinate* y, *and* n *is total data.*

Calculating the covariance of x and y (σxy)

$\sigma xy = \frac{\sum_{1=1}^{n}(x_i-x)(y_i-y)}{n}$ (7) with σxy *is correlation between absis and ordinat*(xy).

Calculating major axis $(a)$and minor axis (b)

$a = 2 \times \sqrt{2} \times \sigma x$ (8) and $b = 2 \times \sqrt{2} \times \sigma y$ (9) where σx *is major axis of ellipse and* σy *is minor axis of ellipse.*

To calculate the orientation angle of error ellipse, we need to compute this equation:

$\theta = \frac{1}{2} tan^{-1}\left(\frac{2\sigma xy}{\sigma xx-\sigma yy}\right)$ (10) where $2\sigma xy$ *is covariance of* x *and* $y, \sigma xx$ *is variance of* x, *and* σyy *is variance of* y.

To complete the understanding of this ellipse error equation, the illustration is shown below.

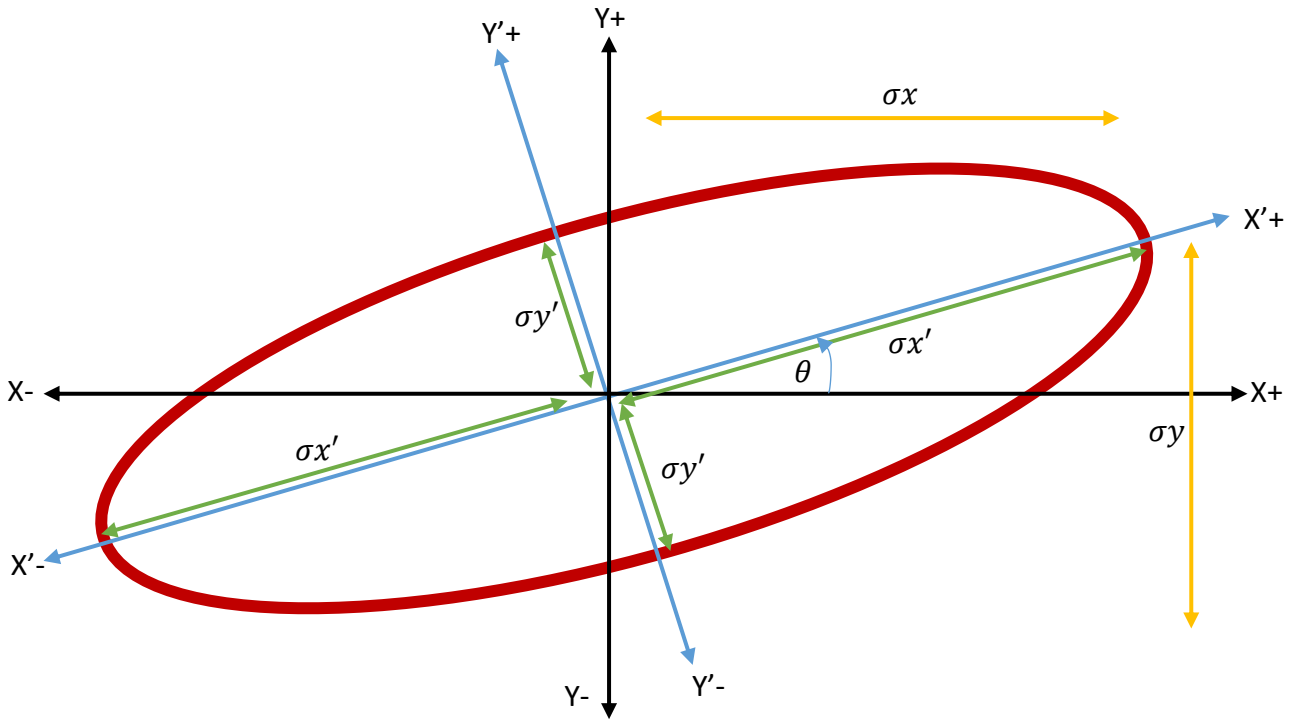

Figure 1. Illustration of Ellipse Error

3. RESULTS

The testing was conducted at twelve sample locations within the campus area of the Indonesian University of Education, encompassing a relatively small geographic extent. These locations included both varied and identical configurations to ensure a comprehensive assessment. The aerial data acquisition was performed at an average flight altitude of approximately 100 meters, following a linear flight trajectory to ensure consistent coverage.The collected aerial imagery was subsequently processed through several photogrammetric stages, including image alignment, feature matching, and georeferencing. During these procedures, intrinsic camera calibration was explicitly applied to ensure the internal parameters of the camera system were accurately accounted for.

DOI: https://doi.org/10.17509/jpis.v32i1.55969
e-ISSN: 2540-7694 p-ISSN: 0854-5251

Following the georeferencing process, an analysis was conducted to evaluate the relationship between intrinsic calibration parameters and georeferencing errors, which were visualized in the form of error ellipses. Twelve distinct samples yielded varying levels of positional error. From each sample, the maximum error values derived from the error ellipse models were extracted and used for comparative analysis against all intrinsic calibration parameters. GCP positions and their associated error estimates are visualized, where the color of each ellipse indicates the error magnitude in the Z direction, while the shape and orientation of the ellipse represent the errors in the X and Y directions. The estimated positions of the GCPs are denoted by dots.

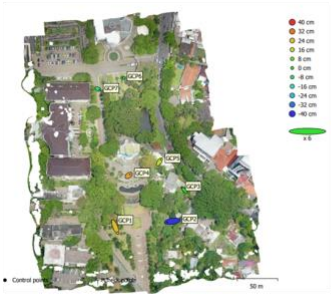

Figure 2a. Sample 1

Figure 2b. Sample 2

Figure 2c. Sample 3

Figure 2d. Sample 4

Figure 2e. Sample 5

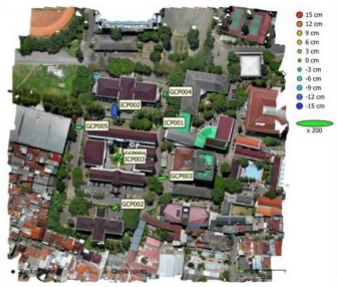

Figure 2f. Sample 6

DOI: https://doi.org/10.17509/jpis.v32i1.55969
e-ISSN: 2540-7694 |p-ISSN: 0854-5251

Figure 2g. Sample 7

Figure 2h. Sample 8

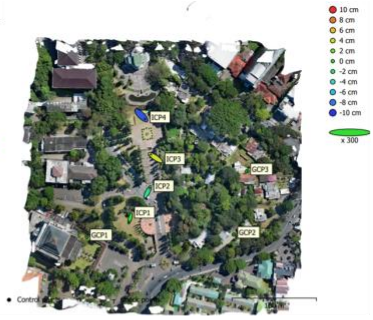

Figure 2i. Sample 9

Figure 2j. Sample 10

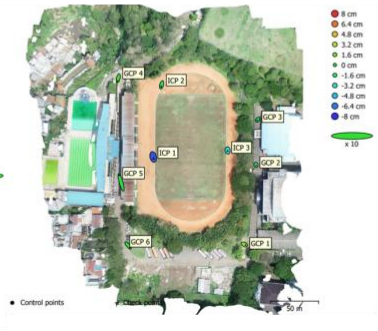

Figure 2k. Sample 11

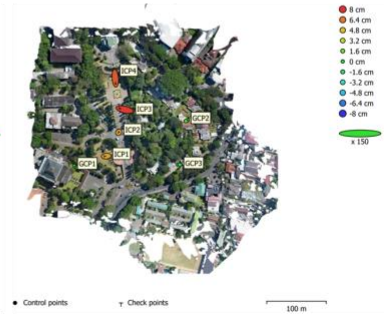

Figure 2l. Sample 12

Figure 2. Figures 2a through 2l present twelve sample data acquisition points, displaying orthophotos alongside error ellipses. The Z-axis error is indicated by the color of the ellipse, while the X and Y errors are represented by the ellipse's shape. Estimated ground control point (GCP) locations are denoted by dots or crosses.

The testing was carried out in four sequential stages. First, an analysis was conducted to examine the correlation between the maximum positional error observed at each sample location and the calibration parameter focal length. Second, a correlation analysis was performed between the maximum estimated GCP error and the principal point coordinates (cx and cy). In the third stage, the relationship between maximum GCP error and the radial distortion coefficients (k1, k2, and k3) was evaluated. Finally, the fourth stage involved analyzing the correlation between maximum GCP error and the tangential distortion coefficients (p1 and p2). Each stage aimed to assess the influence of individual intrinsic calibration parameters on spatial accuracy, as indicated by the maximum error derived from error ellipse models.

DOI: https://doi.org/10.17509/jpis.v32i1.55969
e-ISSN: 2540-7694 p-ISSN: 0854-5251

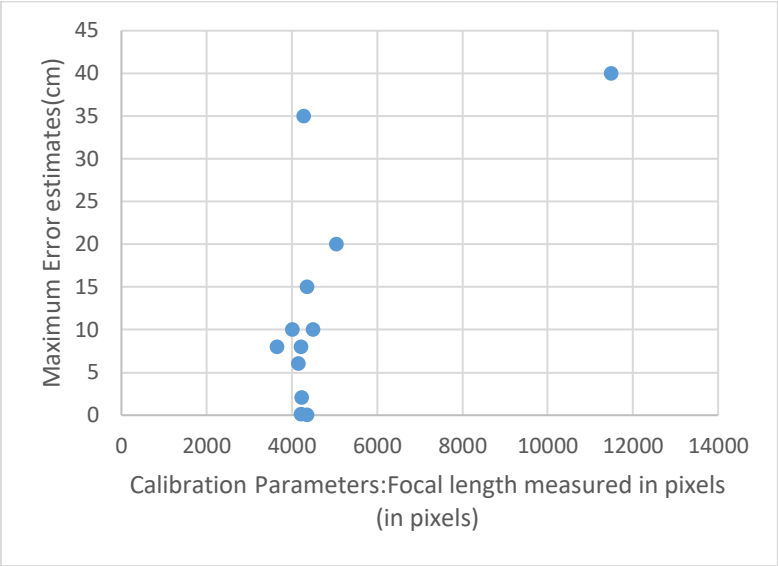

Figure 3. Correlation between maximum error estimation in ground control points (GCP) and the focal length parameter obtained from camera calibration.

Figure 3 illustrates the correlation between the maximum error estimation of Ground Control Points (GCPs) and the focal length, as derived from the processed camera calibration parameters. The graph indicates that the highest precision occurs when the focal length is around 4000, with maximum errors ranging from near zero to approximately 20 centimeters. However, an anomaly is observed at a focal length near 4000, where the error unexpectedly reaches 35 centimeters. The most significant anomaly appears at a focal length approaching 12,000, where the corresponding maximum error exceeds 40 centimeters.

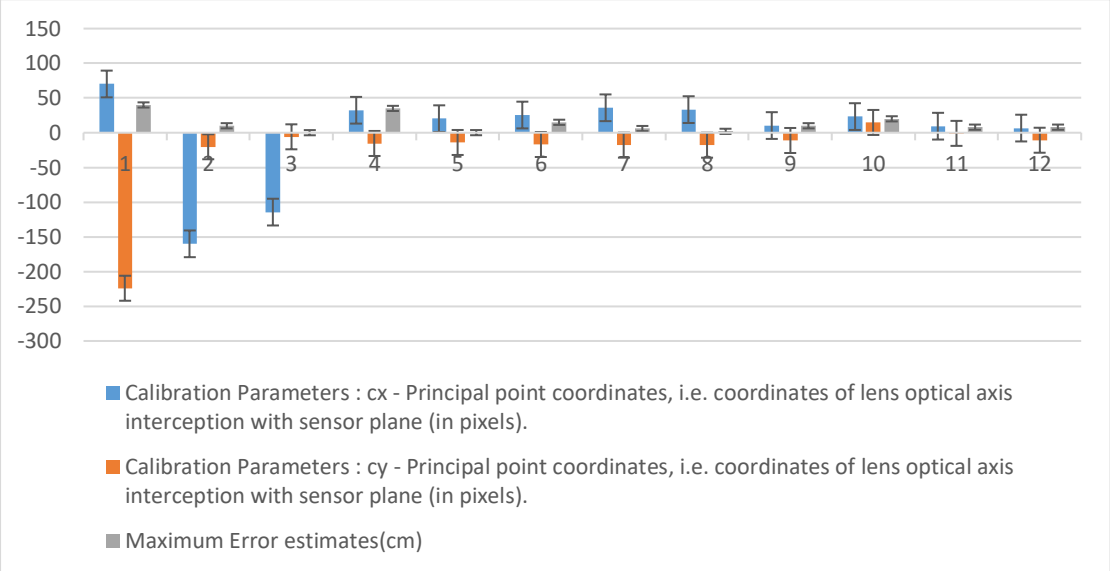

Figure 4. The correlation between maximum error estimation in GCP with Calibration Parameters : cx and cy - Principal point coordinates, i.e. coordinates of lens optical axis interception with sensor plane (in pixels).

The spatial correlation between the principal point coordinates (cx and cy) and the maximum GCP error appears to be relatively consistent across all samples. The analysis shows that higher error values tend to be associated with larger deviations in cx and cy values. This trend is observed consistently throughout the dataset, suggesting a direct relationship

DOI: https://doi.org/10.17509/jpis.v32i1.55969
e-ISSN: 2540-7694 |p-ISSN: 0854-5251

between the magnitude of principal point offsets and the level of georeferencing error. The findings indicate that as the values of cx and cy increase, the corresponding positional error at GCPs also tends to increase proportionally.

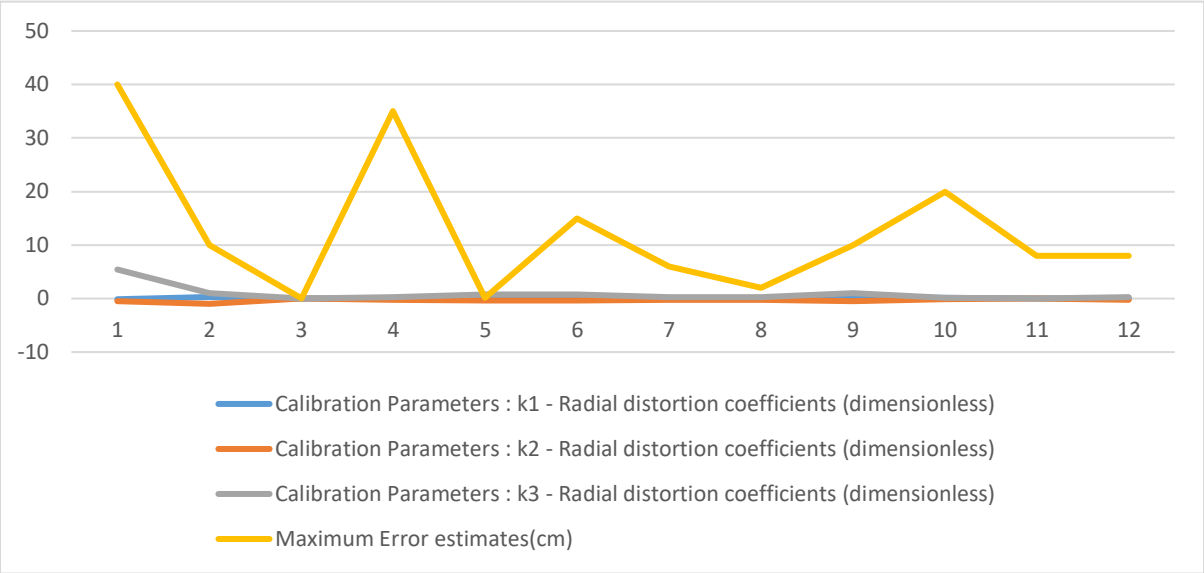

Figure 5. Correlation analysis between maximum ground control point (GCP) error estimation and the radial distortion calibration parameters k_1, k_2, and k_3 (dimensionless).

The analysis presented in **Figure 5**, which investigates the relationship between maximum positional error and radial distortion values derived from internal calibration parameters, presents certain complexities in interpretation. Nonetheless, it is well established that radial distortion significantly affects the geometric integrity of semantic orthophotos. The results of the analysis reveal a dynamic correlation between maximum error values and the magnitude of radial distortion coefficients. Notably, spikes in radial distortion often align with increases in maximum error, and similar decreases occur in tandem—suggesting a reciprocal pattern.

This observation highlights a compelling finding: although the relationship is not strictly linear, the interaction between ground coordinate reference accuracy and radial distortion exhibits a consistent dynamic trend, implying an underlying dependency. This correlation is particularly evident in samples 1, 2, 3, 5, 6, and 9, all of which demonstrate a positive association between elevated radial distortion values and higher georeferencing errors.

The analysis of the relationship between maximum error, as visualized through error ellipses, and GCP residuals in relation to tangential distortion reveals a notably distinct pattern **Figure 6** and **Figure 7**. The data demonstrates a high level of precision for maximum error values below 20 centimeters. However, several anomalies were identified at specific points, warranting further investigation to determine the underlying causes. Interestingly, the tangential distortion coefficients, p1 and p2, exhibited distinct anomalous behaviors that deviated from the general trend.

These findings contribute to the broader discussion on how lens tangential distortion and GCP-related errors can significantly influence the geometric accuracy of the resulting orthophotos. The observed precision in the majority of the dataset, coupled with the emergence of localized anomalies, provides preliminary evidence supporting the hypothesis that tangential distortion plays a meaningful role in the georeferencing process when integrated with GCPs. These results suggest that even subtle lens distortions can introduce measurable positional discrepancies in photogrammetric products.

DOI: https://doi.org/10.17509/jpis.v32i1.55969
e-ISSN: 2540-7694 p-ISSN: 0854-5251

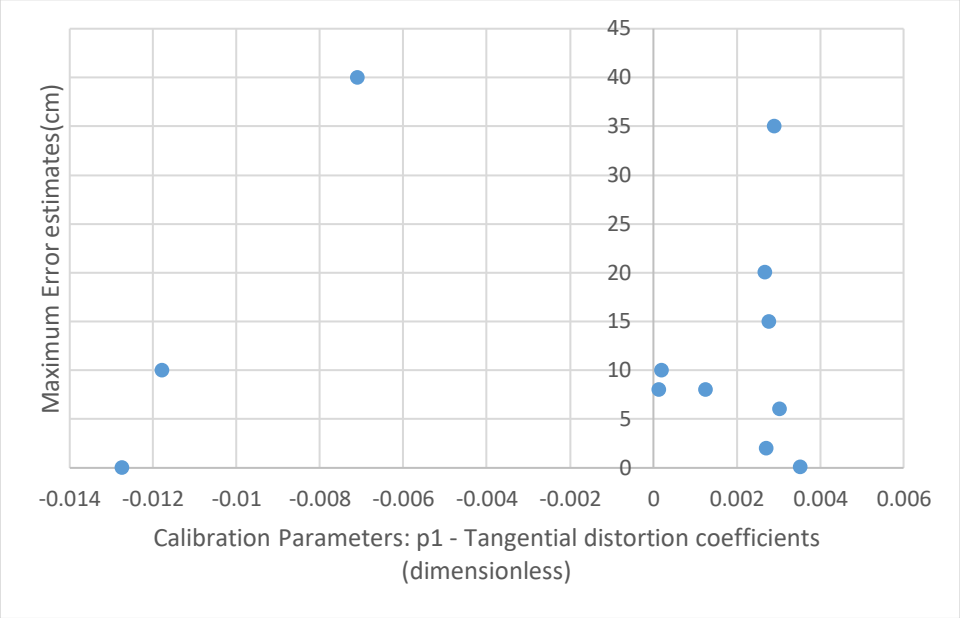

Figure 6. The correlation between the maximum error in GCP estimation and the calibration parameter p1, representing the tangential distortion coefficients (dimensionless).

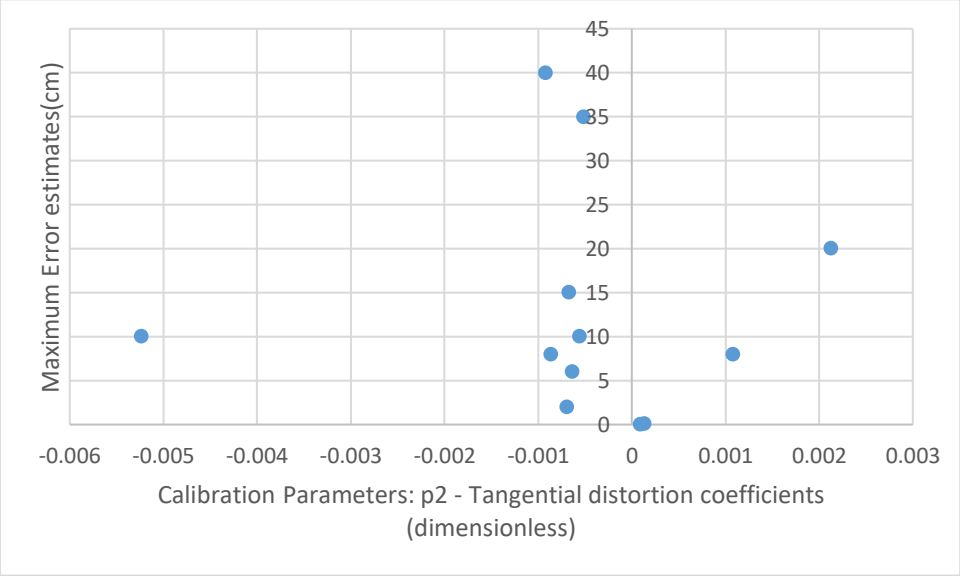

Figure 7. The relationship between the maximum error in GCP estimation and the calibration parameter p2, which represents the tangential distortion coefficients (unitless).

5. ACKNOWLEDGEMENT

The authors would like to express their sincere appreciation to the Study Program of Survey, Mapping and Geographic Information; Geographic Information Science; and Geography Education, Faculty of Social Science Education, Indonesia University of Education for providing the facilities and support that contributed significantly to the successful completion of this research..

6. AUTHORS' NOTE

The authors declare that there is no conflict of interest regarding the publication of this article. Authors confirmed that the paper was free of plagiarism.

4. CONCLUSION

DOI: https://doi.org/10.17509/jpis.v32i1.55969
e-ISSN: 2540-7694 |p-ISSN: 0854-5251

This study has demonstrated that the accuracy of orthophoto products is strongly influenced by intrinsic camera calibration parameters and the spatial distribution of Ground Control Points (GCPs). Through detailed analysis of aerial data collected from twelve sample locations at the Indonesian University of Education campus, the research confirmed that stable camera calibration characterized by consistent focal length and minimal principal point offsets is essential for minimizing positional errors in orthophoto generation. The findings showed that higher stability in these parameters correlates with improved geometric accuracy, underscoring their critical role in photogrammetric workflows.

The investigation into lens distortion effects revealed that both radial and tangential distortions significantly impact spatial accuracy. Increased radial distortion coefficients were generally associated with larger positional errors, highlighting the need for precise distortion correction during camera calibration. Similarly, tangential distortion, though less frequently emphasized in prior studies, showed a measurable influence on positional discrepancies, especially when coupled with suboptimal GCP configurations. These results suggest that even subtle internal camera distortions can propagate into meaningful spatial inaccuracies if not adequately accounted for.

A key contribution of this study lies in its use of error ellipses to visualize and quantify positional uncertainty in two- and three-dimensional spaces. This approach allowed for a nuanced assessment of how calibration parameters and GCP layout jointly affect the shape, size, and orientation of positional error distributions. The application of error ellipses provided clearer insights into spatial error patterns than traditional scalar error metrics alone, facilitating better interpretation of photogrammetric quality and reliability.

4. DISCUSSION

The research highlights the interactive effect between camera calibration quality and GCP distribution. Poorly configured GCP networks exacerbated the impact of calibration deviations, resulting in notable anomalies in error magnitudes. This finding emphasizes that orthophoto accuracy cannot be optimized by focusing solely on either calibration or GCP placement; rather, a holistic strategy incorporating both factors is necessary. Photogrammetric practitioners should prioritize rigorous calibration routines alongside careful GCP network design to ensure the highest positional fidelity. In summary, this study advances the understanding of the multifaceted influences affecting orthophoto accuracy by integrating calibration parameter analysis with spatial error modeling. The demonstrated correlations and error patterns provide practical guidance for improving photogrammetric processing and product quality. Future work should explore dynamic calibration approaches and adaptive GCP placement strategies to further enhance orthophoto precision, particularly in complex terrain or variable operational conditions. Building on these findings, future research should focus on several key areas to further advance orthophoto accuracy and photogrammetric methodologies. The development and testing of adaptive or real-time camera calibration techniques could mitigate the effects of internal mechanical shifts during field operations, especially for nonmetric cameras. Incorporating machine learning models to predict and adjust calibration parameters dynamically based on image content or environmental conditions may enhance robustness. Expanding the scope of this research to include diverse geographic and operational contexts—such as urban environments, mountainous terrain, or multi-sensor aerial platforms—would test the generalizability of the observed relationships between calibration parameters, GCP distribution, and orthophoto accuracy. This would also facilitate the development of tailored calibration and control strategies suited for specific use cases.

DOI: https://doi.org/10.17509/jpis.v32i1.55969
e-ISSN: 2540-7694 p-ISSN: 0854-5251

Finally, investigating the combined influence of other photogrammetric factors such as image matching algorithms, atmospheric conditions, and flight parameters on error ellipse characteristics could provide a more holistic understanding of the sources of positional uncertainty. Such comprehensive analyses would support the refinement of photogrammetric processing pipelines and contribute to improved reliability and precision in geospatial data products.

6. REFERENCES

Bolkas, D. (2020). Matching confidence constrained bundle adjustment for multi-view high-resolution satellite images. Remote Sensing, 810.

Bolkas, D. P. (2023). Review of photogrammetry, remote sensing, and geospatial sciences requirements by various accreditation bodies. The International Archives of the Photogrammetry Remote Sensing and Spatial Information Sciences, 259-265.

Brown, D. C. (1971). Close-range camera calibration. Photogrammetric Engineering, 855-866.

Burdziakowski, P. (2020). Matching confidence constrained bundle adjustment for multi-view high-resolution satellite images. Remote Sensing, 810.

Campos, J. H. (2015). Evaluation of different methods for non-metric camera calibration. ISPRS, 1-8.

Colomina, I. &. (2014). Unmanned aerial systems for photogrammetry and remote sensing: A review. ISPRS Journal of Photogrammetry and Remote Sensing, 79-97.

Forlani, G. D. (2018). Quality assessment of DSMs produced from UAV flights georeferenced with on-board RTK positioning. Remote Sensing, 311.

Fraser, C. S.-A. (2006). Empirical modeling of radial distortion in zoom lenses as a function of focal length. Photogrammetric Engineering & Remote Sensing, 925-933.

Fryskowska, A. W. (2016). Camera calibration performance on different non-metric cameras. Geodesy and Cartography, 195-204.

Garcia, M. V. (2020). The influence of ground control points configuration and camera calibration for DTM and orthomosaic generation using imagery obtained from a low-cost UAV. ISPRS Journals of the Photogrammetry, Remote Sensing and Spatial Information Sciences, 239-246.

Ghilani, C. D. (2018). Adjustment computations: Spatial data analysis (6th ed.). Wiley.

Gindraux, M. e. (2017). Accuracy of UAV photogrammetry in glacial and periglacial alpine terrain: A comparison with airborne and terrestrial datasets. Frontiers in Remote Sensing.

Gui, S. (2024). Advancing applications of satellite photogrammetry: Novel approaches for built-up area modeling and natural environment monitoring using stereo/multi-view satellite image-derived 3D data. The Ohio State University.

Hagemann, A. K. (2021). Inferring bias and uncertainty in camera calibration. arXiv.

Kaamin, M. B. (2023). Production and evaluation of orthophoto map using UAV photogrammetry. Journal of Advanced Research in Applied Sciences and Engineering Technology, 187-196.

Kshirsagar, K. T. (2024). Camera calibration using robust intrinsic and extrinsic parameters. In

DOI: https://doi.org/10.17509/jpis.v32i1.55969
e-ISSN: 2540-7694 |p-ISSN: 0854-5251

Advances in Computer Vision . Taylor & Francis., 123-145.

Lichti, D. D. (2005). Self-calibration of close-range photogrammetric systems. ISPRS , 272-285.

Maalek, R. &. (2020). Automated calibration of mobile cameras for 3D reconstruction of mechanical pipes. arXiv.

Mikhail, E. M. (1981). Surveying and mapping: Theory and application. Harper & Row.

Morgan, M. (2014). Quantitative measures for the evaluation of camera stability. ISPRS Journal of Photogrammetry and Remote Sensing, 1-10.

Okie, E. S. (2020). Detailed geodetic technique procedures for structural deformation monitoring and analysis. International Journal of Scientific and Technological Research, 13-18.

Pessoa, F. A. (2020). The influence of flight configuration, camera calibration, and ground control points for digital terrain model and orthomosaic generation using unmanned aerial vehicles imagery. Brazilian Journal of Cartography, 1-13.

Qiang, Z. J.-j.-q. (2016). The outdoor rapid calibration technique and realization of nonmetric digital camera based on the method of multi-image DLT and resection. ISPRS, 265-269.

Rokhmana, C. A. (2019). Cadastral surveys with non-metric camera using UAV: A feasibility study. Geodesy and Cartography, 157-165.

Şahin, C. (2023). Effect of camera calibration refreshing on orthophoto position accuracy in UAV mapping. Turkish Journal of Remote Sensing and GIS, 83-99.

Sanz-Ablanedo, E. e. (2018). The influence of ground control points configuration and camera calibration for DTM and orthomosaic generation using imagery obtained from a low-cost UAV. ISPRS, 239-246.

Seo, J. L. (2021). Comparative assessment of the effect of positioning techniques and ground control point distribution models on the accuracy of UAV-based photogrammetric production. Sensors, 15.

Shortis, M. R. (1998). Camera calibration for photogrammetry and remote sensing. Photogrammetric Engineering & Remote Sensing, 881-888.

Šidák, Z. (1967). Rectangular confidence regions for means of multivariate normal distributions. Journal of the American Statistical Association, 626-633.

Skarlatos, D. &. (2021). UAV photogrammetry accuracy assessment for corridor mapping based on the number and distribution of ground control points. . Remote Sensing, 2447.

Sobura, S. (2021). Calibration of non-metric UAV camera using different test fields. Geodesy and Cartograph, 111-117.

Tjahjadi, M. E. (2019). Assessing stability performance of non-metric camera's lens distortion model during UAV flight missions. KnE Engineering, 345-354.

Tournadre, J. e. (2020). UAV photogrammetry accuracy assessment for corridor mapping based on the number and distribution of ground control points. MDPI Remote Sensing, 2447.

Viswanathan, S. (2005). Photogrammetric error sources and impacts on modeling and surveying in construction engineering applications. Visualization in Engineering, 2(2).

Yusoff, A. R. (2015). The effect of varies camera calibration fields on camera parameters. Jurnal

DOI: https://doi.org/10.17509/jpis.v32i1.55969
e-ISSN: 2540-7694 p-ISSN: 0854-5251

Teknologi (Sciences & Engineering), 1-7.

Yusoff, M. Z. (2017). Performance evaluation of non-metric digital camera for photogrammetric application. Journal of Surveying Engineering.

Zhang, Y. C. (2023). Camera calibration demystified: A step-by-step guide to obtaining intrinsic and extrinsic parameters and correcting lens distortion. Medium.

Zhang, Z. (2000). A flexible new technique for camera calibration. IEEE Transactions on Pattern Analysis and Machine Intelligence, 1330-1334.

Zhao, Z. L. (2021). UAV photogrammetry accuracy assessment for corridor mapping based on the number and distribution of ground control points. . Remote Sensing.

Zhou, Y. R.-D. (2020). Simulation and analysis of photogrammetric UAV image blocks: Influence of camera calibration error. Remote Sensing, 22.

DOI: https://doi.org/10.17509/jpis.v32i1.55969
e-ISSN: 2540-7694 |p-ISSN: 0854-5251